# Research of Situ Strain of Measuring Flexible Truss Deformation Based on Fuzzy Network Method

Yong Zhao[1], Hong Bao[1, a, *], Xuechao Duan[1] and Hongmei Fang[2]

[1]Key Laboratory of Electronic Equipment Structure Design of Ministry of Education Xidian University, Xi'an 710071, China;

[2]Nanjing Research Institute of Electronics Technology, Nanjing 210039, China.

[a] hbao@xidian.edu.cn

**Abstract.** An adaptive fuzzy network method is proposed for measuring flexible truss deformation by using situ strain in this paper. The relation matrix between strain and arbitrary deformation nodes of truss is first derived by using inverse finite element method. Based on the elements of matrix, strain measuring displacements are obtained. In addition, an adaptive fuzzy network for measuring truss deformation is developed according to the measured displacement and situ strain. Furthermore, the experiment on deformation measurement of the flexible truss modal is conducted. The experiment shows that the adaptive fuzzy network measuring method is characterized by high accuracy for measuring flexible truss deformation.

**Keywords:** Flexible truss; Strain selection; Inverse finite element method; Adaptive fuzzy net; Deformation measuring.

## 1. Introduction

A Due to light mass, strong bearing and easy adjustment, the flexible truss has been widely used in smart structures such as the wings of unmanned air vehicle (UAV), large deploy-able antennas in satellites and the bracket of array antenna [1]. Nevertheless, the flexible truss tends to bend and twist when bearing temperature and external loads. For example, the wings of UAV are distorted under the influence of air-stream in cruising, which will not only cause harm to the flight safety, but also decrease the pointing accuracy of array antennas of radar conformed on the wings. In this case, the wings of UAV need real-time feedback to the control system and actuator with real-time deformation measuring to maintain a safe flight [2]. Moreover, the deformation quantities are used to correct the excitation current or provide feedback to actuator to adjust initial phase distribution of the array antennas with the purpose of ensuring the pointing accuracy and gain of antennas [3]. Therefore, the real-time measuring of flexible truss deformation plays an important role in structures health monitoring. However, for the truss deformation measurement in aerospace, the present main method is still measuring the situ strain with strain sensors to estimate the situation of the entire structure.

In the literature [4-6], the global or piecewise continuous basis function methods were employed to fit surface measured strain into structure strain field, and then the structure deformation displacement was obtained from the strain-displacement relationship. This method is easy to implement, but its range of application and accuracy of deformation estimation depend on the appropriate selection of basis function and weight coefficients. Modal shapes are used as basis function in [7, 8]. The deformation displacements are reconstructed from measured strains by using the modal transformation method. However, there exist the following disadvantages in this method: 1) The detailed material elasticity and inertial parameters are needed to precisely construct modal shapes; 2) This method is difficulty to tackle with geometrically nonlinear problems. For example, the flexible truss of the aircraft wings has different modal shapes under different loads so a single modal shape cannot accurately reflect structure deformation.

On the basis of Euler-Bernoulli beam equation, R.Glaserd and Ko et al determined the deflection of beam by the integration of discretely measured strains directly[9,10]. Particularly, Ko et al applied the classical beam equation to develop a kind of method to approximate beam curvature through integrating the discrete measured strains [10]. Their one-dimensional solution has displayed high accuracy in predicting deflection, but this method fails to estimate the element deformation under multidimensional complex loads.

Tessler and Spangler [11] reconstructed the shear-deformable structures of plates and shells using the inverse finite methodology (IFEM), which is able to reconstruct three-dimensional displacement vector from surface measuring strains in all the domains according to the least-square variance principle. Due to the fact that only the displacement-strain relationship is used, this methodology conducts deformation reconstruction can be accomplished without the prior knowledge of loads, materials and inertial damping. FBG sensors were applied in [12] to measure the surface strains on the slender beams and then the deformation displacement was reconstructed by using an iFEM shell model. The beam deformation displacement and cross-section torsion were reconstructed by Gherlone et al who employed the inverse finite element method to achieve high reconstruction accuracy of deformation displacement without any prior knowledge of the finite element modal and loads in [13-14]. Nevertheless, the scheme ignores that the installation errors of the strain sensors have influence on the deformation estimating. Moreover, the large curvature has harmful effect on the measuring accuracy of the sensors stuck on the special angle positions.

Feng et al developed a deformation measurement algorithm based on fuzzy network [15]. In their solution, the displacement of the measured points and the strain data of the involved points are trained with fuzzy network to determine the relationship between displacement and strains. In the applied phase of network rules, the strain measured values of the involved points are used as the network input data and then deformation displacement values of measured nodes are directly obtained through the trained network. Because the fuzzy network train of the non-linear relationship is carried out according to deformation displacement values of the concerned points and the measured data of the relevant strains, the consequent accuracy highly depends on the selection of the relevant strains. Therefore, the optimized selection of the relevant strain needs to be firstly conducted before applying this method.

On the basis of situ strain selection, this paper presents an adaptive fuzzy network methodology to measure the flexible truss deformation. The relation matrix, which indicates the relation between situ strain and the arbitrary measured nodal of truss, was derived by IFEM firstly. And the situ strain will be selected according to the relation matrix. Furthermore, the nonlinear relationship between the displacement and the strain will be obtained based on the measured nodal deformation and the selected situ strain data with adaptive fuzzy network. Eventually, the experiment is carried out on the fabricated flexible truss in order to validate the effectiveness of the measuring system.

## 2. The Selection of Situ Strain Nodes

For the common optimal methods for transducer selection [16, 17] such as Effective Independence (EI), Modal Kinetic Energy (MKE), it is the structure modal shape obtained from the kinematic equation that is optimized. The optimization objective is the typical active nodes in mode shape or the measurement points that can reflect the maximum Fisher information matrix of mode shape.

However, the optimization of the above methods depends tightly on the accuracy of establishing finite element model of the structure. Since it is no need of the prior knowledge such as finite element model of structure and loads, the IFEM is employed to optimally select strain in the paper.

The IFEM [14] determines the relationship between the nodal kinematic variables and any measured cross-section in the beam element by estimating the least-square error between the theoretical strains and the experimental strains:

$$\mathrm{k^e u^e = f^e} \tag{1}$$

$k^e$, $f^e$ are defined as follows:

$$k^e = \sum_{k=1}^{6} w_k k_k^e \qquad f^e = \sum_{k=1}^{6} w_k f_k^e$$
$$k_k^e = \frac{L}{n}\sum_{i=1}^{n}[B_k^T(x_i)B_k(x_i)]$$
$$f_k^e = \frac{L}{n}\sum_{i=1}^{n}[B_k^T(x_i)e^{\varepsilon i}] \tag{2}$$

Where $\mathrm{u^e}$ denotes nodal kinematic variables, $\mathrm{B(x)}$ is the coefficient matrix that involves the derivatives of the shape function, L denotes the length of the beam element, $\mathrm{e^{\varepsilon i}}$ and n are the section strains and its number respectively in the element; $n = 1$ in this paper, the section strains are obtained by computing the measured surface strain:

$$\varepsilon_x^*(x_i,\theta,\beta) = e_1(x_i)\left(c_\beta^2 - v s_\beta^2\right) + e_2(x_i)\left(c_\beta^2 - v s_\beta^2\right)s_\theta R_{ext} + e_3(x_i)\left(c_\beta^2 - v s_\beta^2\right)c_\theta R_{ext} + e_4(x_i)c_\beta s_\beta c_\theta - e_5(x_i)c_\beta s_\beta s_\theta + e_6(x_i)c_\beta s_\beta R_{ext} = A * e^{\varepsilon i}(u) \quad (3)$$

In (3), $v$ is the passion ratio, $e^{\varepsilon i}(u)$ and $\varepsilon_x^*(x_i,\theta,\beta)$ are the section strains and measured surface strains, respectively. $R_{ext}$ Denotes the distance between the centroid of the section and the location of the situ strain. Then, $A$ can be considered as the coefficient matrix transferring the cylindrical coordinate to Cartesian coordinate.

In the finite element framework, the element kinematic field can be interpolated by nodal kinematic variables and shape function:

$$u(x) \cong u^h(x) = N(x)u^e \quad (4)$$

Where, $N(x)$ *d*enotes the shape function and $u(x)$ is the element kinematic field.

Substituting Eq. (2) into Eq. (1) results in the following form of Eq. (3):

$$u(x) = N(x)(k^e)^{-1}f^e \overset{n=1}{\Longrightarrow} N(x)(k^e)^{-1}\left(\sum_{k=1}^{6} w_k\left[B_k^T(x_i) * \left(A^{-1}\varepsilon_x^*(x_i,\theta,\beta)\right)\right]\right) = T * \varepsilon_x^*(x_i,\theta,\beta) \quad (5)$$

Thus, each component in $u(x)$ can denote the weighted sum of the measurement surface strain.

$$u_i^e = a_{i1}e^{\varepsilon_1} + a_{i2}e^{\varepsilon_2} + \cdots + a_{ik}e^{\varepsilon_j} \quad (6)$$

Where, $u_i^e \in u^e$ denotes the nodal kinematic variables component. $j$ is the number of mounted sensors, and $e^{\varepsilon_i} \in \varepsilon_x^*(x,\theta,\beta)$ is surface strain value obtained from $i^{th}$ strain sensor. $a_{i1}, a_{i2}, \ldots, a_{ik} \in T$ Refer to the weights of the displacement component directly corresponding to the strain value. The contribution of every strain measurement point when calculating deformation displacement can be determined thought comparing the absolute values of the weights. For instance, if the absolute value of one weight is larger, its strain value of the point is closely related to deformation displacement. This strain value can thus be selected as the input data of the network. Otherwise, the strain value of the measurement point should be abandoned. Based on the above-mentioned rule, the measured nodal strains are optimally selected.

Table 1. Location of strain sensors

| $e^{\varepsilon_1}(x,\theta,\beta)$ | $e^{\varepsilon_2}(x,\theta,\beta)$ | $e^{\varepsilon_3}(x,\theta,\beta)$ | $e^{\varepsilon_4}(x,\theta,\beta)$ | $e^{\varepsilon_5}(x,\theta,\beta)$ | $e^{\varepsilon_6}(x,\theta,\beta)$ |
|---|---|---|---|---|---|
| $(L/2,-2\pi/3,0)$ | $(L/2,-2\pi/3,\pi/4)$ | $(L/2,0,0)$ | $(L/2,0,\pi/4)$ | $(L/2,2\pi/3,0)$ | $(L/2,2\pi/3,\pi/4)$ |

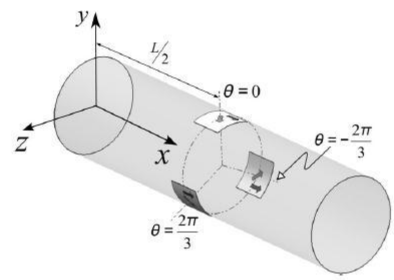


Fig. 1 Placement of strain sensors in beam element

For the different inverse frame elements, the number of the transducers and the components of $e_1, e_2, \ldots, e_6$ are accordingly different in Eq. (3). For the $0^{th}$-order element, section strains $e_i$ (*i=1*, *4-6*) are constant and $e_i$ (*i=2*, *3*) are linear, thus six strain sensors are required. While for the $1^{st}$ -order element, the sections strains $e_1$ and $e_6$ are constant, $e_4$ and $e_5$ need to be linear, $e_2$ and $e_3$ parabolic, thus eight strain sensors are required. The $0^{th}$-order element is chosen in this paper and location of strain sensors will be laid in the table 1.

## 3. A Fuzzy Net for Measuring Flexible Truss

The measuring method of the adaptive fuzzy network includes the two stages as follows: training stage of strain-displacement relationship in fuzzy network and its application stage. The training will start after determining the most relevant strains corresponding to the selected displacements.

There are four procedures in the training stage of the adaptive fuzzy network: Adding membership functions and rules; Deleting membership function and rules; Tuning of the consequents of adaptive ruler; Solidifying the rule base. They are described in detail as follows.

### 3.1 Adding Membership Functions and Rules

On the basis of systematic current error (root mean square (RMS) error in this paper) and *ε*-completeness (*ε=0.5*), we can judge whether the fuzzy network need add the membership function or not. The membership function will be added if the current systematic current error is greater than the default or the minimum value less than the default ε in the corresponding maximum membership degree of all the input data.

In the process of generating rules, the membership function of the maximum membership degree in the current input strain data is defined as the antecedent of the rule and the corresponding deformation displacement will be regarded as the consequent of the rule. One rule is created every time. A rule could be denoted as Eq. (7) assuming that one nodal of the beam element at one certain moment is associated with *N* strain values:

$$\text{Rule i: IF } x_1 \text{ is } A_1^{i_1} \text{ and } x_2 \text{ is } A_2^{i_2} \ldots x_N \text{ is } A_N^{i_N}, \text{THEN } y = a_i \tag{7}$$

Where, $A_v^{i_v} \in \{A_v^1, A_v^2, \ldots, A_v^{n_v}\}$ is the membership function of the maximum membership degree of the input strain hereinafter; $n_v$ and $a_i$ are the number of membership function of the input strain and consequent of $i^{th}$-rule, respectively. Thus, the displacement output of the nodal at *k* moment is:

$$Y = \frac{\sum_{i=1}^{N_{rules}} a_i \mu_i(\vec{x}(k))}{\sum_{i=1}^{N_{rules}} \mu_i(\vec{x}(k))} = \sum_{i=1}^{N_{rules}} a_i \emptyset_i \tag{8}$$

Where, $\vec{x}(k) = \left(x_1(k), x_2(k), \ldots, x_N(k)\right), N_{rules}$ , and $\mu_i$ are the number of fuzzy rules and activation degree of $i^{th}$-rule, respectively.

### 3.2 Deleting Membership Functions and Rules

Adapter deletion for membership functions and rules is added in fuzzy network to avoid the problems such as computation complexity increasing and learning efficiency decreasing due to increasing the membership functions and rules blindly. $C_i$ And $S_i$ are defined as the rate of contribution of rule and deletion index, respectively:

$$C_i = \frac{|y_i|}{\sum_{i=1}^{N_{rules}} |y_i|} \tag{9}$$

$$S_i = \begin{cases} S_i'\tau & if \quad C_i < \beta \\ S_i' & if \quad C_i \geq \beta \end{cases} \tag{10}$$

Where, $y_i = a_i \emptyset_i$, $S_i'$ is the value at the previous step, $\tau(0<\tau<1)$and β are attenuation factor and threshold of update, respectively. $S_i$ Is initialized to 1, default the deletion threshold, δ. The rule should be deleted under the condition that $S_i$ is less than . The nodal of the adjacent membership function should be adjusted in time after the rule is deleted with the purpose of maintaining the distribution continuity of the membership functions.

### 3.3 Tuning of the Consequent of Adaptive Ruler

When the error of the current deformation displacement due to estimating and measuring is relatively large, the consequent of the rule should be adjusted with reward and penalty:

$$\Delta a_i(k) = \sigma * \mu_i(k-1)\left(r(k-1) - y(k)\right) \tag{11}$$

where, $\Delta a_i(k)$ denotes the adjusted consequent of the rule at *k* moment; $\mu_i$(k-1) and r(k-1) are the activation of $i^{th}$-rule and the measured deformation displacement at $k-1$ moment, respectively; y(k) is the estimated displacement of the system at the current *k* moment; σ is a constant for tuning the rule; the value of this constant has effect on adjusting the convergence rate of strategy and displacement accuracy of net output.

### 3.4 Solidifying the Rule Base

When the training of the adaptive fuzzy network can meet the given precision, the rule base of the current strain-displacement relationship is saved. After that, the deformation displacements of the measured nodal points at the given precision will be acquired through the saved rule base, which input data are the corresponding strains associated with the measured nodal points (Fig.2).

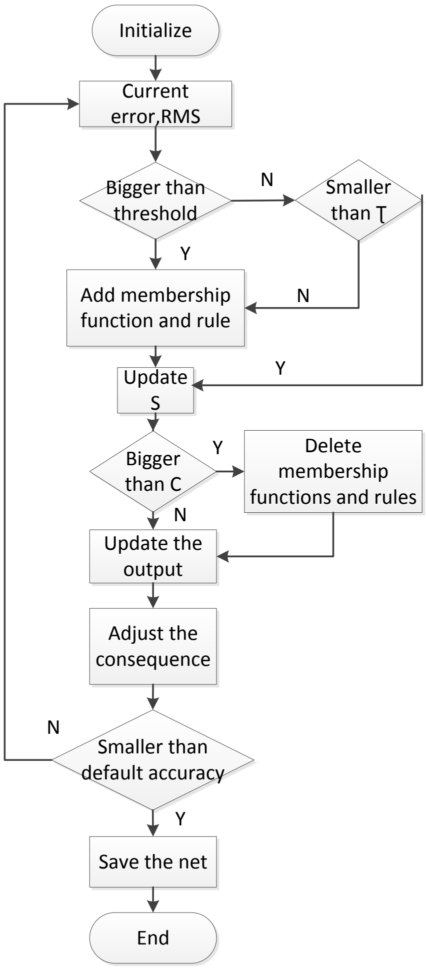


Fig. 2 The flow chart of training the adaptive fuzzy net

## 4. Experimental Validation

The 2m truss under the excitation of different static loads is analyzed to evaluate the accuracy of the proposed fuzzy network measured methodology. The truss structure is made of aluminum alloy, which Young's modulus is Poisson ratio is 0.3, density is 2557*KG/m*$^3$ and the radius of the girder is 7 *mm*. The truss deformation displacements and strains information are gathered by the strain collected system and the displacement collected system respectively (Fig.3).

Fig.3 Measured system and truss (A. Displacement collected; B. Truss; C. Strain collected)


Fig.4 Truss and loads (A. Load; B. Girder)

The strain collected system is composed of strain gauge, amplifier and signal collection board and the displacement collected system is composed of the dynamic 3D optical measurement instrument with high precision (NDI Optrotrak ertus).The girder of the truss is divided into six elements. Because the strain gauges can be placed anywhere along the beam surface, their distributions for every element in this paper are summarized in Table 1.

The free end of the truss girder is statically loaded by a series of different concentrated loads (Table 2). Regarding the zero loading as the zero of the measurement system, the corresponding strains and displacements are derived under different loads. From the total 19 sets of loaded data (Fig.4),12 sets are selected randomly and then imported into the adaptive fuzzy network, which are trained to obtain the rule base of strain-displacement relationship.

As the applied data, the remainder 7 sets of data will be used to validate the effectiveness of the fuzzy network. The loads are shown in Table 2. Every set of data comprises of 10 strain values and 10 displacement values selected randomly from the measured system.

Table 2. Loading (KG)

| | 1 | 2 | 3 | 4 | 5 | 6 | 7 | 8 | 9 | 10 | 11 | 12 |
|---|---|---|---|---|---|---|---|---|---|---|---|---|
| Train | 1 | 1.2 | 1.8 | 2.2 | 3.2 | 3.7 | 5 | 5.2 | 5.6 | 6.4 | 7 | 7.5 |
| Test | 0.6 | 1.6 | 3 | 4.3 | 4.8 | 6 | 7.3 | | | | | |

To verify the effectiveness of the fuzzy network, the deformation displacement accuracy of the first beam element of the girder is measured because there are the same structure and material for every element of the truss (As shown in Fig.5). The transformation relation of displacement-strain is deduced by inputting the length of the beam element, the material parameter, the pasted location of strain gauges and the measured nodal point of displacement (the right node in the element) into Eq. (5).

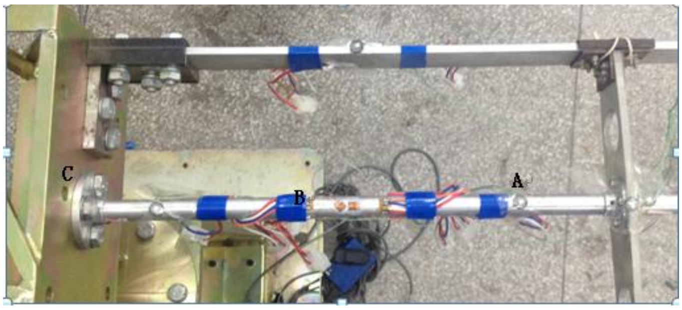

Fig. 5 The first beam element and its measurement points (A. The measured nodal point of displacement; B. Location of section strain and strain gauge; C. Constraint)

Table 3. Transformational relation matrix of displacement-strain

| $T$ | $e^{\varepsilon_1}$ | $e^{\varepsilon_2}$ | $e^{\varepsilon_3}$ | $e^{\varepsilon_4}$ | $e^{\varepsilon_5}$ | $e^{\varepsilon_6}$ |
|---|---|---|---|---|---|---|
| $u$ | 0.1163 | 0 | 0.1163 | 0 | 0 | 0 |
| $v$ | 0.371 | -0.116 | -0.717 | 0 | 0.347 | -0.116 |
| $w$ | 0.586 | 0.067 | 0.014 | -0.134 | -0.64 | 0.067 |
| $\theta_x$ | -11.63 | 33.24 | -11.63 | 33.24 | -11.63 | 33.24 |
| $\theta_y$ | -28.83 | 0.003 | 0.0017 | -0.0059 | 28.83 | 0.003 |
| $\theta_z$ | 16.64 | 0.005 | -33.29 | 0 | 16.65 | -0.005 |

In Table. 3, $u$, $v$ and $w$ denote the displacements at $y = z = 0$; $\theta_x$, $\theta_y$ and $\theta_z$ are the rotations about the three coordinate axes (Fig.4). In the table, the sum of the three weights of strain sensor locations $e^{\varepsilon_1}$, $e^{\varepsilon_3}$ and $e^{\varepsilon_5}$, represent about 100%, 86.1%, 82.2%, 26%, 99.8% and 99.98% in six kinematic variables, respectively. The focus is put on the corresponding strain displacements associated with three displacement components, $u, v$ and $w$ as the current displacement measured system can only get the displacement without the rotations. For displacement of the vertical direction, $w$ , the absolute of the weight of $e^{\varepsilon_4}$ is slightly greater than $e^{\varepsilon_3}$. Moreover, the curvature of the external beam surface due to small error of strain measured, $e^{\varepsilon_3}$ is still chosen as input data of fuzzy network instead of$e^{\varepsilon_3}$.

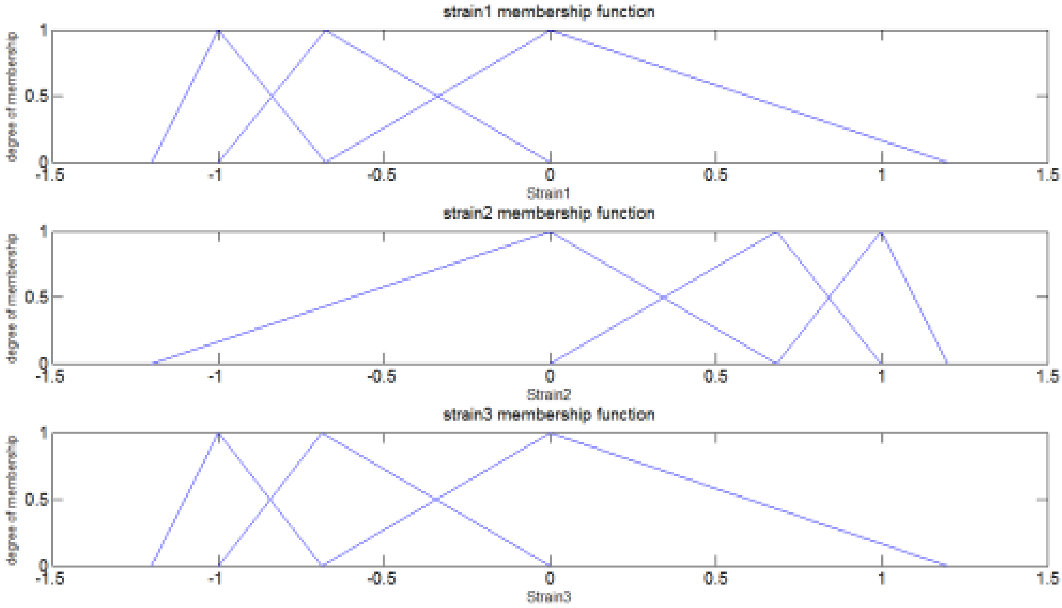

Fig. 6 Distribution of membership function of strain

The distribution of the membership functions of the selected three strain values in fuzzy network are shown in Fig.6, and the system errors between the measured displacements and displacements that deduced in training and application stages of the fuzzy network are shown in Fig. 7(a~ c). The error of displacement between the measured and fuzzy network deduced along y axis is less than that along the other two axes. The errors are about 0.19 mm in training stage and 0.2 mm in application stage, respectively. However, the errors along z axis are greater than x and y axes, the errors about 1.7 mm in training stage and 1.77 mm in application stage, respectively. The reason is the direction of the static loads along z axis, and the main deformation of the truss girder is the vertical down bending, thus the relative displacement in vertical is much greater than the other two directions. Moreover, it is important to observe the error tend figures that the error between actual measured and fuzzy network deduced decreases with the deformation displacement increasing, and the applicability of using the fuzzy network to measure the large deformation of flexible truss has been illustrated.

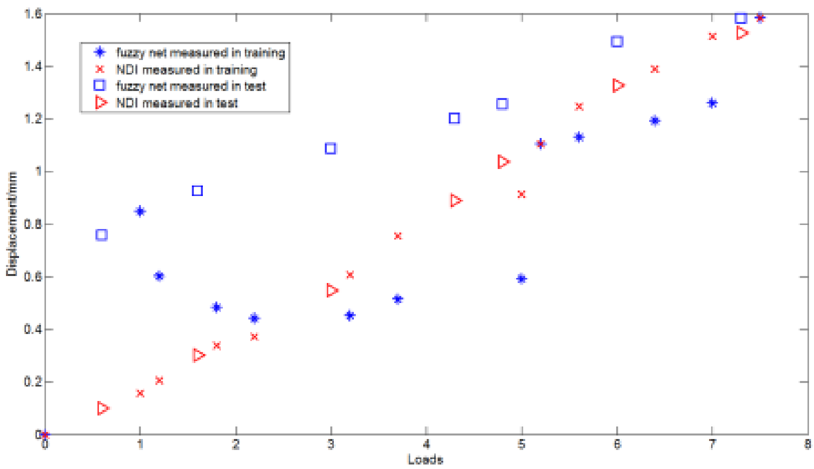

Fig. 7a Error of displacement u in fuzzy net training stage

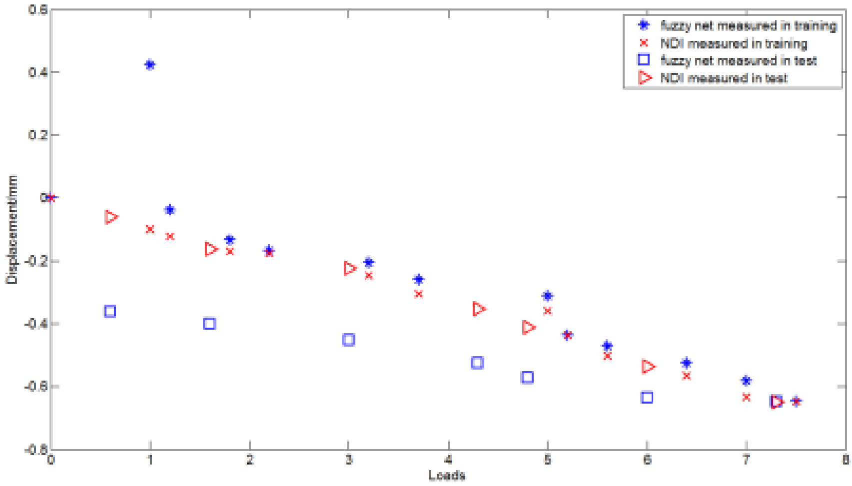


Fig. 7b Error of displacement v in fuzzy network

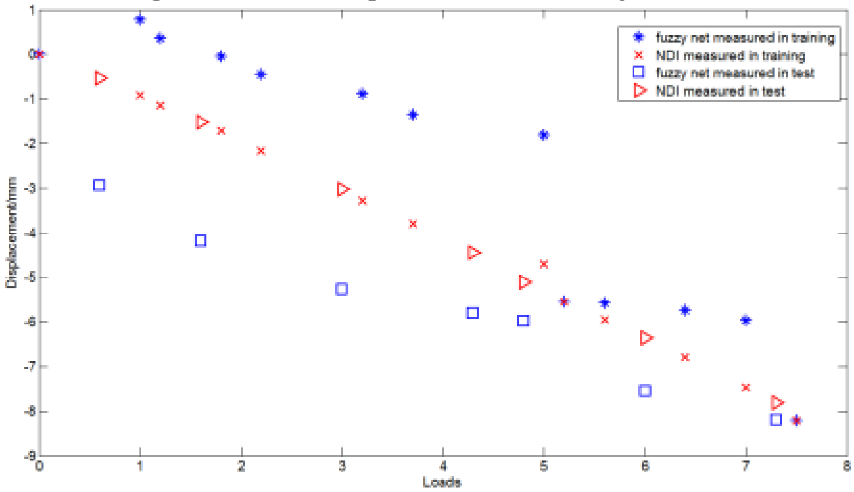


Fig. 7c Error of displacement w in fuzzy network

The deformation displacement error of the first three beam elements in direction *Z* is obtained by using the fuzzy network method to measure the second and third elements of the girder (Figure.4). The errors in network's training and application stages are 4.23 mm and 4.58 mm, respectively (Table.4).

Table 4. Errors of deformation displacement of the first three elements

| | Training error of *w* | Implication error of *w* |
|---|---|---|
| 1-st element | 1.70mm | 1.77mm |
| 2-nd element | 4.66mm | 4.32mm |
| 3-rd element | 5.39mm | 6.42mm |
| The first three elements | 4.23mm | 4.58mm |

It can be found that the error between the displacement deduced by the fuzzy network and the actually measured displacement increases with the sequence number of the girder element increasing. This is mainly because the distance between the beam element and the fixed constraint increases with the sequence number of the girder element increasing. Moreover, combing with the gap between the joints of elements, the strain of the element decreases. Then, the nodal displacement of the beam element was influenced by the prior element rotation primarily. Meanwhile, since the $4^{th}$ beam element, the displacement led by the prior element rotation will be the main factor to affect the current element (Figure.8). Therefore, an important problem to be solved will be how to delete the influence produced by beam element deeply before the network training.

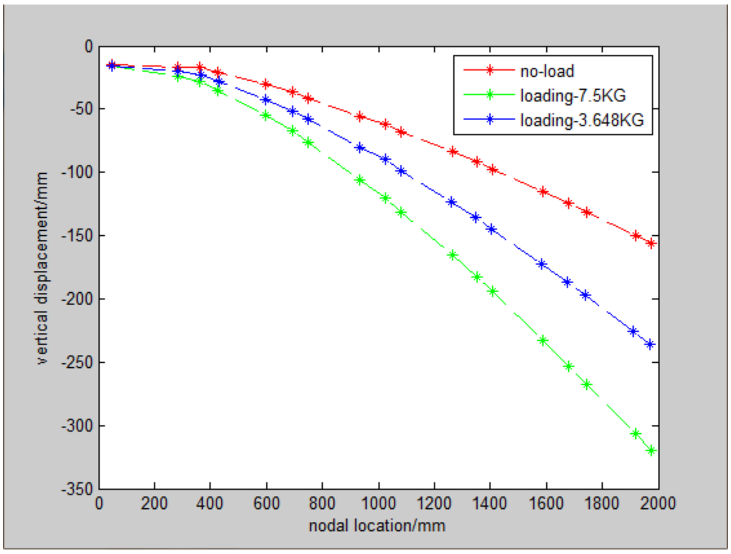


Fig.8 Deformation displacement of girder in direction Z

## 5. Conclusion

In search of a suitable algorithm for use in real-time recovering the deformation of the truss, an adaptive fuzzy network method has been formulated to perform the shape-sensing of 3D truss structures undergoing static deformation. The fuzzy network trains the displacement-strain relationship by using the selected nodal displacement and the strain measured data selected optimally by IFEM.

The experiment shows that the proposed fuzzy network method has a high accuracy in estimating the deformation of truss girder element in the fixed constraint and loads. But with the distance between the element and the constraint increasing, the relation between the strain and displacement is weakened gradually. The displacement produced by the element rotation increases predominantly due to decreasing the accuracy of the network training. Therefore, the future work will make focus on how to reduce the error brought by the element rotation and how to increase the accuracy of recovering the deformation of the truss structure.

## References

[1] Tieliang Zhang, Yunliang Ding, Haibao Jin, et al. Multi-objective optimization design for trusses of spacecraft antenna. Chinese Journal of Solid Mechanics, 2012, 33(6):603-610.

[2] Chen Guohai. Technologies for Next Generation Airborne Early Warning Radar. Modem Radar, 2010, 32(3):1-4.

[3] Zeng Xiangneng, He Feng, et al. Analysis and compensation of space-bone SAR antenna array deformation. Journal of National University of Defense Technology, 2012, 34(3):158-163.

[4] Foss G and Haugse E. Using modal test results to develop strain to displacement transformation. Proc. 13th Int. Conf. Modal Anal. (Nashville, TN, Feb.1995) pp: 112-118.

[5] Peter S Lively, Mauro J Atalla, Nesbitt W Hagood. Investigation of filtering techniques applied to the dynamic shape-estimation problem. Smart Materials and Structures. 2001, 10(2):264-272.

[6] M.D.TODD, S.T.VOHRA. Shear deformation correction to transverse shape reconstruction from distributed strain measurements. Journal of Sound and Vibration. 1999, 225(3):581-594.

[7] Philip B. Bogert, Eric Haugse, Ralph E. Gehrki. Structural shape identification from experimental strains using a modal transformation technique. 4th AIAA/ASME/ASCE/AHS Structures, Structural Dynamics, and Materials Conference 7-10 April 2003, Norfolk, Virginia.

[8] Kim, Hong-Il, Kang, Lae-Hyong, et.al. Shape estimation with distributed fiber Bragg grating sensors for rotating structures. Smart Materials and Structures. 2011, 20(3):35011-35021.

[9] R. Glaser, V. Caccese, M. Shahinpoor. Shape Monitoring of a Beam Structure form Measured Strain or Curvature. Experimental Mechanics. 2012, 52(6):591-606.

[10] Ko W L, Rochards W L and Fleischer V T. Applications of the Ko displacement theory to the deformed shape predictions of the doubly-tapered Ikhana wing. NASA Technical Paper. NASA/TP-2009-214652.

[11] Tessler A and Spangler J L. A Least-squares variational method for full-field reconstruction of elastic deformations in shear-deformable plates and shell [J]. Comput. Methods Appl. Mech. Eng. 2005, 194:327-339.

[12] Vazquez S L, Tessler A, Quach C C, Cooper E G, et al. Structural health monitoring using high-density fiber optic strain sensor and inverse finite element methods. NASA Technical Paper. NASA/TM-2005-213761.

[13] Gherlone M, Cerracchio P, Mattone M, Di Sciuva M and Tessler A. Dynamic shape reconstruction of three-dimensional frame structures using the inverse finite element method. NASA Technical Paper. NASA/TEP-2011-217315.

[14] Gherlone M, Cerracchio P, Mattone M, Di Sciuva M and Tessler A. Shape sensing of 3D frame structures using an inverse Finite Element Method [J]. International Journal of Solids and Structures. 2012, 49:3100-3112.

[15] FENG Siyuan, BAO Hong, ZHANG Xudong. An Airfoil Antenna Deformation Measurement Method Based on Fuzzy Network. Modern Radar. 2015, 37(11):59-63.

[16] SHAH P C, UDWADIA F E. A Methodology for Optimal Sensor Locations for Identification of Dynamic Systems. Journal of Applied Mechanics, 1978, 45(1): 188-196.

[17] C.S. Kubrusly, H. Malebranche. Sensors and controllers location in distributed systems- a survey. Automatica 1985, 21:117-128.

[18] M. Papadopoulos, E. Garcia. Sensor placement methodologies for dynamic testing. American Institute of Aeronautics and Astronautics. 1998, 36(2):256-263.

[19] WORDEN K, BURROWS AP. Optimal Sensor Placement for Fault Detection. Engineering Structures, 2001, 23(8): 885-901.

[20] KAMMER D C. Sensor Placement for On-orbit Modal Identification and Correlation of Large Space Structures. IEEE. Proceedings of the 1990 American Control conference. San Diego: IEEE, 1990:251-259.

[21] YAO L, SETHARES W A, KAMMER D C. Sensor Placement for On-orbit Modal Identification via a Genetic Algorithm. AIAA Journal, 1993, 31(10): 1922-1928.

[22] WANG L, ZHENG D Z. An Effective Hybrid Optimization Strategy for Job-shop Scheduling Problems. Computers& Operations Research, 2001, 28(6):585-596.

[23] LI Shou-ju, LIU Ying-xi, FENG Ying. Identification of the Damping Coefficients in Dynamic System Using Hybrid Genetic Algorithm. Chinese Journal of Computational Mechanics, 2004, 21(5): 551-556.